We are IntechOpen,
the world's leading publisher of
Open Access books
Built by scientists, for scientists

5,600
Open access books available

137,000
International authors and editors

170M
Downloads

154
Countries delivered to

Our authors are among the

TOP 1%
most cited scientists

12.2%
Contributors from top 500 universities

BOOK CITATION INDEX
CLARIVATE ANALYTICS
INDEXED

WEB OF SCIENCE™

Selection of our books indexed in the Book Citation Index
in Web of Science™ Core Collection (BKCI)

Interested in publishing with us?
Contact book.department@intechopen.com

Numbers displayed above are based on latest data collected.
For more information visit www.intechopen.com

Chapter

Vertical Bearing Capacity of Precast Pier Foundation Filled with Demolished Concrete Lumps

Bin Lei, Wengui Li, Zhuo Tang and Fuzhi Yang

Abstract

The application of recycled compound concrete made of demolished concrete lumps (DCLs) and fresh normal concrete in pier foundation can effectively improve the utilization efficiency of construction waste resources. In this study, two prefabricated pier foundations based on recycled compound concrete (dimension of Ø800 × 2500 mm and Ø1000 × 2500 mm) and two cast-in-place pier foundations based on ordinary concrete (dimension of Ø800 × 2500 mm and Ø1000 × 2500 mm) were tested. Special attention was devoted to the load-settlement curve characteristics of the precast pier foundation of compound concrete, the load transfer law of the pier-soil system, the soil pressure distribution at the bottom of the pier, and the failure mode. The results showed that the Q-S curve of precast concrete pier foundation made of recycled compound concrete is slow deformation at loading, which is consistent with that of cast-in-place concrete pier foundation. The load transfer theory of pier-soil system is established, and its accuracy is verified by experimental analysis. The precast foundation of recycled compound concrete is the same as the cast-in-place foundation of ordinary concrete. The failure form of prefabricated pier foundation made of recycled compound concrete was a local shear failure, while the failure form of ordinary concrete cast-in-place pier foundation was piercing-type shear failure. The feasibility of relevant theoretical methods for calculating the vertical ultimate bearing capacity is examined.

Keywords: recycled compound concrete, demolished concrete lump, pier foundation, vertical bearing capacity

1. Introduction

With the growing interest in sustainable and environmentally friendly construction, recycled aggregate concrete (RAC) has been widely investigated and is gradually being incorporated into real engineering projects [1–4]. A series of investigations has been conducted around the world on the mechanical properties, durability, and structural performance of RAC [2, 5–7]. Adopting demolished concrete blocks (DCBs) rather than recycled aggregates in structural members may reduce the cost of reuse of waste concrete. DCBs have distinctly larger size than the conventional recycled aggregates [8–11]. Therefore, the utilization of construction and demolition waste has great significance in saving resources, protecting the

environment, and realizing the sustainable development of the construction industry. Combined with the favorable geological conditions of Nanchang city, this paper made a preliminary exploration on casting large-size demolished concrete lumps (DCLs) and fresh concrete, e.g., recycled compound concrete, into pier foundation, which was used as a new type of building foundation form.

The research on pier foundation was first carried out in the United States, followed by the former Soviet Union, Japan, and other countries. In particular, a large number of experimental results were obtained in the research on pier foundations with enlarged bottom [12]. The experimental research on pier foundation in China is relatively lagging behind. The theoretical research on pier foundation is more than the experimental research, mainly because it requires a large amount of financial and personnel resources to carry out the test. In terms of theoretical research, it mainly focuses on the soil failure theory [13], the design of pier foundation [14], the law of load transfer [15, 16], and the formula for calculating ultimate compressive bearing capacity [16–19]. As for experimental study, it includes the research on end resistance reduction [20], settlement deformation [21, 22], working mechanism [23–26], and bearing capacity formula [25, 27, 28]. Based on the experimental result and theoretical analysis, the paper provides a basis for the research on the vertical bearing capacity of the precast pier foundation with compound concrete.

In general, pier foundation is a kind of foundation form between rigid independent foundation and manual bored pile foundation [27, 29]. In multistory buildings, when the upper shallow foundation soil is relatively good and no weak layer beneath, when compared with shallow foundation, the artificial dig-hole pile foundation does not have the economic advantage, as it needs to use shallow foundation excavation of earthwork, which results in the high cost [27]. However, the pier foundation has good seismic performance, large single pier bearing capacity, and less earthwork excavation [28]; it can meet the design requirements of the building, and the foundation cost is low [29]. Hence, the research on the precast pier foundation made from recycled compound concrete has important engineering application value.

In this study, two prefabricated pier foundations based on recycled compound concrete (dimension of Ø800 × 2500 mm and Ø1000 × 2500 mm) and two cast-in-place pier foundations based on ordinary concrete (dimension of Ø800 × 2500 mm and Ø1000 × 2500 mm) were tested. Special attention was devoted to the load-settlement curve characteristics of the precast pier foundation of compound concrete, the load transfer law of the pier-soil system, the soil pressure distribution at the bottom of the pier, and the failure mode, and then the vertical bearing capacity of precast pier foundation filled with demolished concrete lumps is analyzed.

2. Geotechnical characteristics

The area is located in Jiangxi vocational technical college campus, Nanchang, Jiangxi province. The standard penetration test and the origin of a heavy dynamic penetration test were conducted to investigate the geotechnical characteristics. The soil samples collected by three apertures are shown in **Figure 1**.

According to the analysis of drilling soil samples in engineering geology, the soil stratigraphy consists of two main layers: Holocene filling soil (Q_4^{ml}) and Holocene alluvial layer (Q_4^{al}). According to its lithology and engineering characteristics, the distribution of each soil layer in the survey depth is described as follows:

Layer 1: silt (Q_3^{al}), brown and yellow, hard plastic, local hard, slightly dry, dry strength low, low toughness, shaking response medium, dull, components for clay,
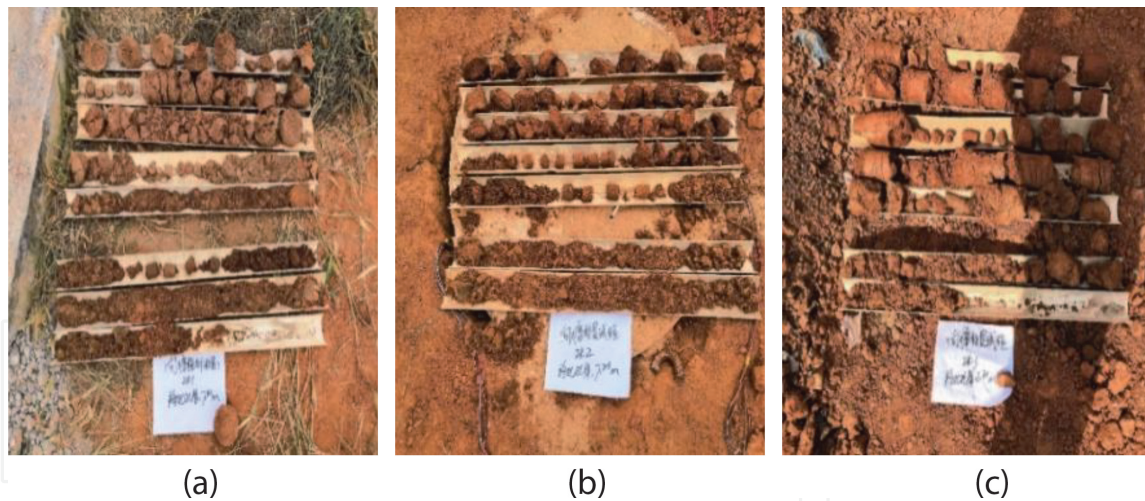
Figure 1.
Soil samples collected from the test sites. (a) ZK$_1$, (b) ZK$_2$, and (c) ZK$_3$.

Soil layer name and number	Characteristic value of bearing capacity (kPa)	Soil heavy (KN/m^3)	Compression modulus E$_s$/deformation modulus E$_0$ (MPa)	Bored pile (clean bottom, D = 800 mm)	
				Ultimate lateral friction q$_{sik}$ (kPa)	Extreme resistance q$_{pk}$ (kPa)
Silty soil	150	18	5.5/	50	—
Medium sand	160	18	/9.0	40	800

Table 1.
Suggested values of physical and mechanical parameters of bedrock soil layer.

sand. The layer thickness is 0.40–1.80 m, and the depth of the top layer is 0.00 m, distributed throughout the field

Layer 2: middle sand (Q$_3$^{al}), brown and yellow, loose to slightly dense, slightly wet, particle composition is mainly quartz, the upper part contains more shale, exposed layer thickness 5.40–5.90 m, layer top buried depth 0.40–1.80 m, distributed throughout.

The main soil properties of each soil layer, derived from the geotechnical investigation, and the evaluation of in situ and laboratory tests are presented in **Table 1**.

3. Experimental procedures

3.1 Raw materials

3.1.1 Concrete

Commercial concrete was used in this study as the fresh concrete, with the mix proportions shown in **Table 2**. The concrete used had a cement content of 220 kg/m^3, a water-cement ratio of 0.46, and a maximum aggregate grain size of 31.5 mm. The slump was 180 mm, and the compressive strength was 35.2 MPa.

Water-cement ratio	Water (kg/m³)	Cement (kg/m³)	Coarse aggregate (kg/m³)	Fine aggregate (kg/m³)	Fly ash (kg/m³)	Water reducer (kg/m³)
0.46	108	220	1050	872	120	6.3

Table 2.
Mix proportions of commercial concrete.

(a)   (b)   (c)
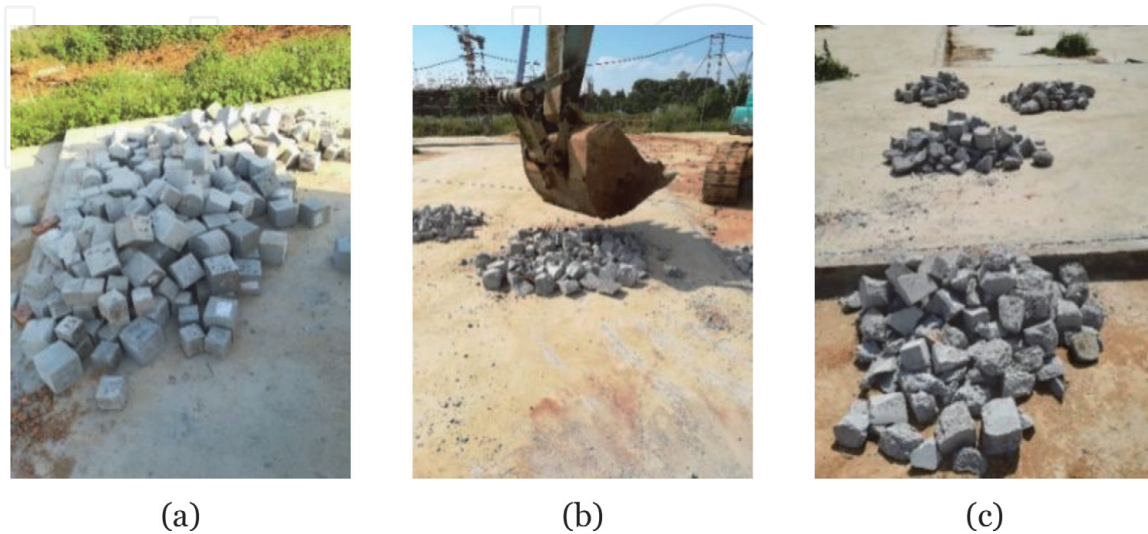
Figure 2.
Demolished concrete lumps. (a) Demolished concrete cubes, (b) crushing by an excavator, (c) concrete lumps selection.

3.1.2 Demolished concrete lumps

The DCLs used in the present study were obtained from the same batch of 150 mm cubic concrete samples reserved in the laboratory for more than 2 years. The cubic compressive strength of DCLs was 30.1 MPa. The demolished concrete cubes from an engineering quality inspection center were broken into lumps by excavator, as shown in **Figure 2**. Only concrete lumps with the sizes of 40–60 mm and 60–80 mm were selected for the inclusion into the recycled compound concrete, and these chosen lumps were used directly in the recycled compound concrete, i.e., without any further processing.

3.1.3 Reinforcement details

As shown in **Figure 3**, HRB 335 bar with a diameter of 12 mm was used for longitudinal bars of the pier foundation, while HRB 335 with a diameter of 8 mm was used for transverse reinforcement with a spacing of 250 mm. Four steel reinforcement cages were made, as shown in **Figure 3**, to serve as the structural reinforcement of the four pier foundations. Two of the piers are 800 mm in diameter and the other two are 1200 mm in diameter. All the four piers are 2400 mm in height. The longitudinal bar selected is HRB335 hot rolled thread steel bar with a diameter of 12 mm. The stirrup is the same type of steel reinforcement with a diameter of 8 mm, including 8 Φ 12 mm and longitudinal reinforcement stirrup Φ 8 @ 250 mm.
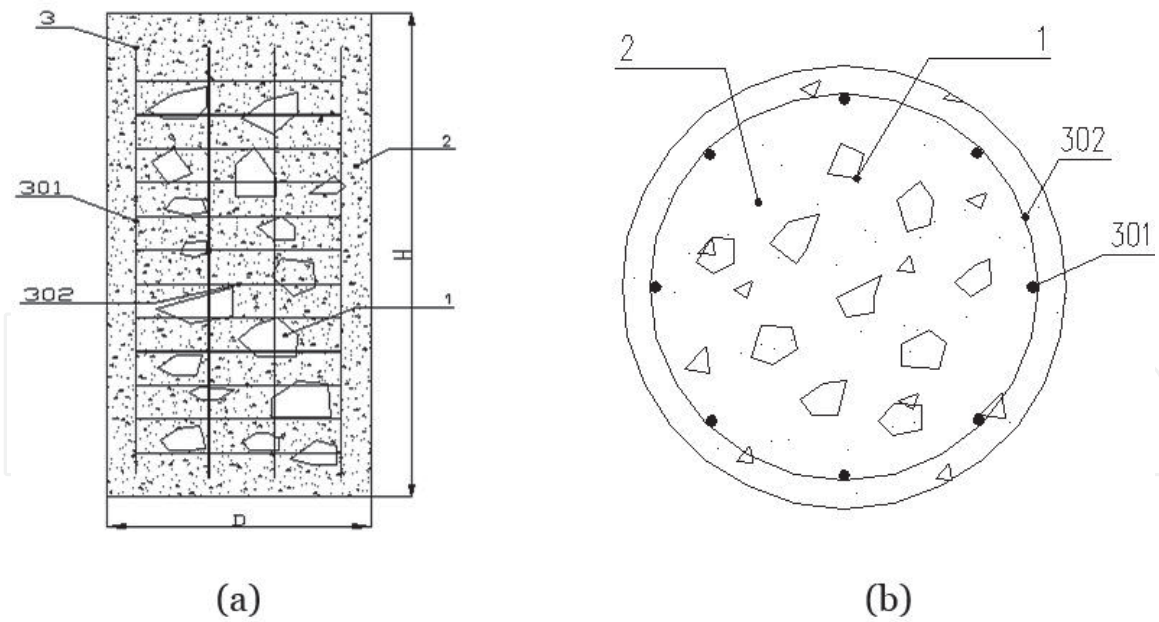
Figure 3.
Steel reinforcement cage.

Figure 4.
Molds for concrete casting.

3.1.4 Concrete molds

Concrete molds were prepared from wood, as shown in **Figure 4**, one with an inner diameter of 800 mm and a height of 2500 mm and the other with an inner diameter of 1000 mm and a height of 2500 mm.

Figure 5.
Schematic diagram of precast pier foundation design (1, DCLs; 2, fresh concrete; 3, reinforcement; 301, longitudinal reinforcement; 302, transverse reinforcement). (a) Longitudinal section, (b) cross-section.

Notation	Count	Dimension (mm × mm)	DCLs grading	$f_{cu,new}$ (MPa)	$f_{cu,old}$ (MPa)	η (%)
YD800	1	∅800 × 2500	40–60 mm:60–80 mm = 6:4	35.24	C25	30
YD1000	1	∅1000 × 2500				
XD800	1	∅800 × 2500	—	35.24	—	—
XD1000	1	∅1000 × 2500	—			

Note: YD800 refers to the precast pier foundation of compound concrete with a diameter of 800 mm. XD1000 refers to the cast-in-place concrete pier foundation with a diameter of 1000 mm.

Table 3.
Details of pier foundations.

3.2 Pier foundation preparation

A total of four pier foundations were prepared, including two precast pier foundations filled with DCLs and fresh concrete (pier foundation dimension: ∅800 × 2500 mm, ∅1000 × 2500 mm) and two ordinary concrete cast-in-situ pier foundation (pier foundation dimension: ∅800 × 2500 mm, ∅1000 × 2500 mm. The schematic diagram of precast pier foundation design is shown in **Figure 5**. The details of pier foundations are presented in **Table 3**.

For pier foundations made of recycled compound concrete (YD1000 and YD800), the replacement rate of DCLs was 30%, and the ratio of DCLs with diameters of 40–60 mm to 60–80 mm was 6:4. The precast pier foundation was cast near the test site. After 28 days of curing, the pier foundations were transported to the construction site. In order to ensure the lifting of the pier foundations during transportation, it is necessary to embed the lifting rings in the pier foundations before they are cast. As suggested in the literature [30], the bending center diameter of the lifting ring was set as 63 mm, the burial depth was set at 75 mm, and the bending hook was set as 25 mm. The casting process of the pier foundation is as follows:

1. Prepare reinforcement cages with diameters of 0.7 and 0.9 m for the pier foundations with diameters of 0.8 and 1.0 m, respectively. Strain gauges were pasted on the longitudinal reinforcement, and the layout of the strain gauges are presented in **Figure 6**. Moreover, the strain gauges were pasted to the outer sides of the longitudinal bars to prevent damage of the strain gauge during concrete casting and vibration.

2. Assemble and splice the wood mold with an inner diameter of 0.8, 1 m, and length of 2.5 m, and drill a hole with diameter 50 mm at the upper part of the mold as the outlet of strain gauge cables.

3. When the height of the mold was 2.5, scaffolding was set up for construction in the casting project. On the one hand, it could fix the mold; on the other hand, it could serve as an operating platform during the concrete casting process.

4. Put the steel reinforcement cage into the mold, and adjust the spacing between the steel reinforcement cage and the mold that there was a 50 mm gap between. The DCLs were wetted before casting to prevent the DCLs from absorbing too much water in the casting process. The fresh concrete is first casted to the bottom of the mold with a height of 250 mm as a cushion. The fresh concrete incorporation with the DCLs with the replacement rate of 30% was casted into the mold. During the casting process, the handheld vibrator is used for continuous vibration. When the casted layer reached 500 mm high, a steel wire mesh with a diameter slightly smaller than the diameter of the steel wire cage was laid on the fresh concrete. Repeat and alternate the above casting process until the mold is filled. The schematic diagram for the height setting of layered steel mesh is shown in **Figure 7**. The steps for the


(a)   (b)
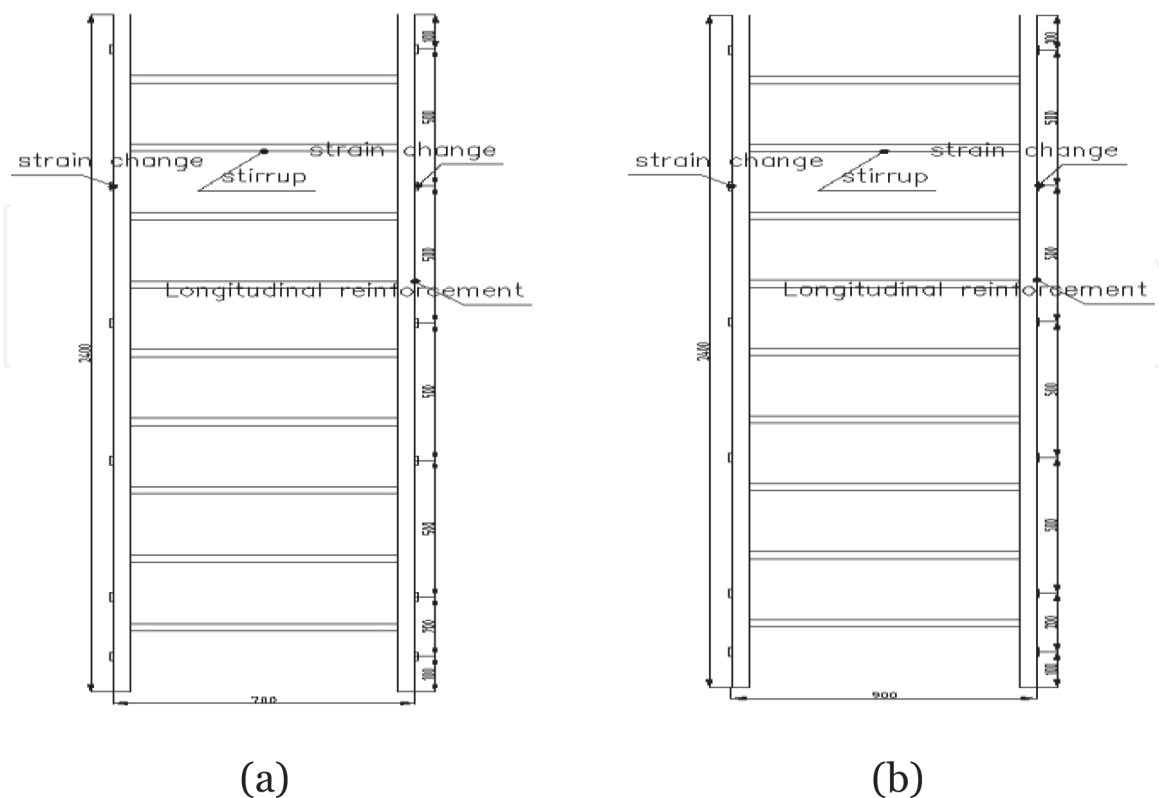
Figure 6.
Layout of strain gauge. (a) Pier foundations of YD800 and XD800, (b) pier foundations YD1000 and XD1000.

preparation of recycled compound concrete and ordinary concrete piers are shown in **Figures 8** and **9**, respectively. After 1 day of curing, the concrete was demolded. Carpet saturated with water was used to wrap the surface of the pier foundations. After 28 days of curing, the pier foundation was lowered into the hole, a little larger than the pile diameter.

5. The gap between the precast pier foundation and the hole shall be backfilled and compacted with undisturbed soil. At the same time, the hanging ring of the precast pier top was sawed off with the cutting machine to ensure the levelness of the pier top.

6. As the two cast-in-place piers of ordinary concrete are casted on the foundation, the pier foundation preparation is as follows. The test hole was dug firstly. Then, the steel cage was lowered into the hole, which was followed by fresh concrete casting. After casting, cover the top of the pier foundation with plastic film to prevent water evaporation.
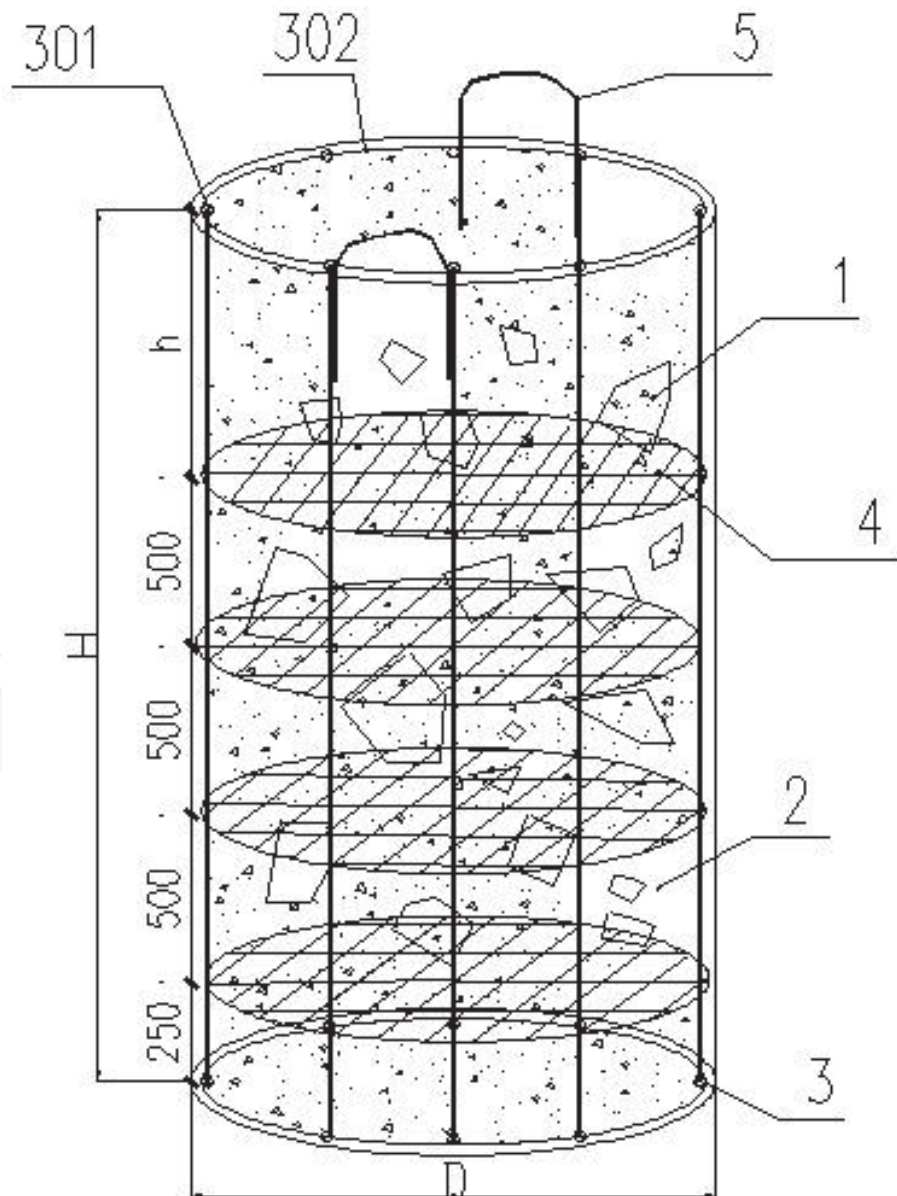
Figure 7.
Schematic diagram of the casting process (1, DCLs; 2, ordinary concrete; 3, reinforcement; 301, longitudinal reinforcement; 302, transverse reinforcement; 4, steel wire mesh; 5, rings).

Figure 8.
Construction steps of precast pier foundation filled with DCLs and fresh concrete for foundation casting. (a) Prepare reinforcement, (b) install mold, (c) set up scaffolding and molds, (d) put the steel cage into the mold, (e) cast new concrete at the bottom of the mold and then place a steel wire mesh, (f) cast new concrete incorporated with concrete lumps to the predetermined height, (g) consolidate concrete, (h) place the second layer of wire mesh, (i) cast new concrete with concrete lumps to the predetermined height and then consolidate, (j) follow steps h and i until the mold is filled, (k) demold after 1 day of curing, (l) cure pier foundation, (m) lower pier foundation into the hole, (n) fill the gap between prefabricated pier foundation and hole with undisturbed soil, (o) saw off the lifting ring to ensure the levelness of pier top end.
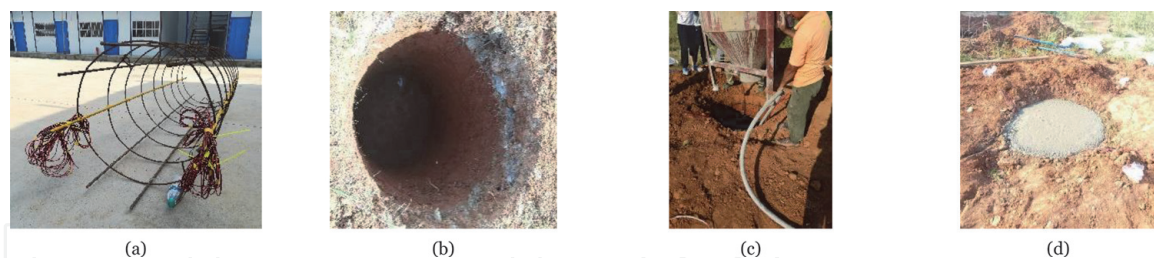
Figure 9.
Construction steps of cast-in-place ordinary concrete piers for foundation casting. (a) Prepare reinforcement; (b) manually dig the hole; (c) put the steel cage into the hole, followed by concrete casting and consolidation; (d) seal the top with membrane to prevent evaporation of water.

3.3 Testing setup

The commonly used reaction methods for vertical compression and static load test of pier foundation include the platform reaction beam method, anchor pile reaction beam method, and anchor pile reaction beam loading method [31]. Based on the actual situation of the site, the platform reaction beam method was adopted in this study, as shown in **Figure 10**. Load counterforce device consisted of the bearing plate, reaction beam system, 320 tons of double oil jack, and 63 MPa ultrahigh pressure pump station. Load counterforce device could provide the reaction force not less than 1.2 times of maximum load value. The load was applied at a rate of movement corresponding to a stress rate on the pier foundation as specified in the code [32]. The compression force was measured by a static load tester (type: RS-JYB), along with the settlement measured by two displacement sensors. To
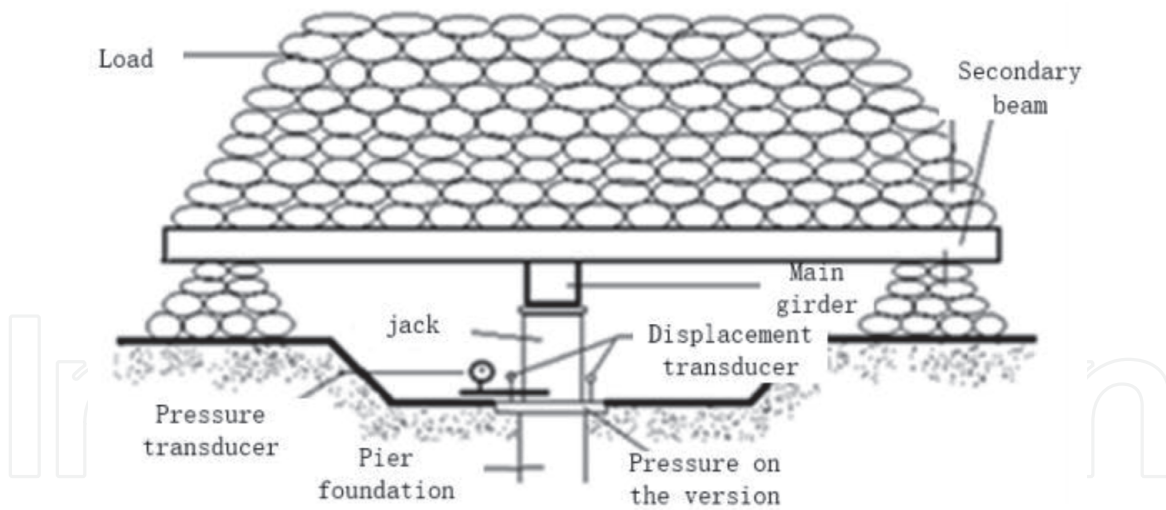
Figure 10.
Test setup.

Model	Dimension	Scale range	Resolution (% F.S.)	Temperature measurement range (°C)	Temperature measurement precision (°C)
JTMV2000	Ø117 × 28 mm	0–2.5 MPa	≤ 0.08	−25 to 60	0.5

Note: F.S. refers to the full range of the equipment.

Table 4.
Parameters of earth pressure gauges.
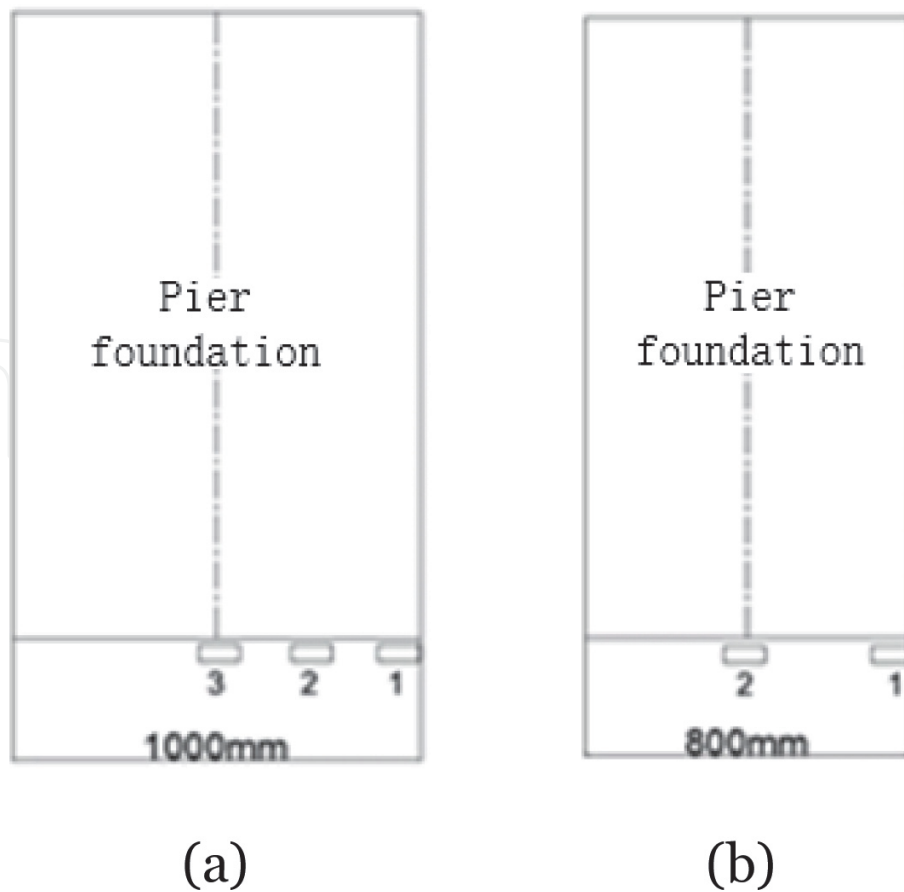

(a)   (b)

Figure 11.
Arrangement of earth pressure boxes. (a) Pier foundation with a diameter of 1000 mm, (b) pier foundation with a diameter of 800 mm.

understand the stress distribution along the pier foundation, six pairs of strain gauges were arranged along with the longitudinal reinforcement, as shown in **Figure 6**. To understand the soil pressure distribution of the foundation, the vibrating wire pressure sensors (JTM-v2000) were applied. The parameters of the sensor are shown in **Table 4**. The vibrating wire pressure sensors were arranged at 100 mm intervals at the bottom of the pier foundation, and the distribution of the earth pressure at the bottom of the pier foundation can be measured by considering half of the symmetrical arrangement. Two earth pressure boxes are required for the diameter of 0.8 m, and three earth pressure boxes are required for the diameter of 1 m. The detailed installation of vibrating wire pressure sensor is shown in **Figure 11**.

4. Results and analysis

4.1 Load-settlement relationship

The measured load-settlement relationships are plotted in **Figure 12**, and the characteristic values are listed in **Table 5**. All the pier foundations exhibit similar load-settlement curves, which belongs to slow variation. According to the geotechnical characteristic measured, the bearing layer of the pier foundation test was located in the middle sand layer, which is consistent with the Q-S curve characteristics of sandy soil [33]. Regardless of the type of pier foundation (recycled compound concrete or ordinary concrete), the characteristic value of vertical bearing capacity of single pier increases with the increase of the diameter of pier foundations. For pier foundations with the same diameter, the vertical bearing capacity of the recycled concrete precast pier is lower than that of the ordinary concrete pier by 25–35%. This is mainly because ordinary concrete was cast-in-situ, and therefore there was relatively large friction between the pier foundation and the soil, while
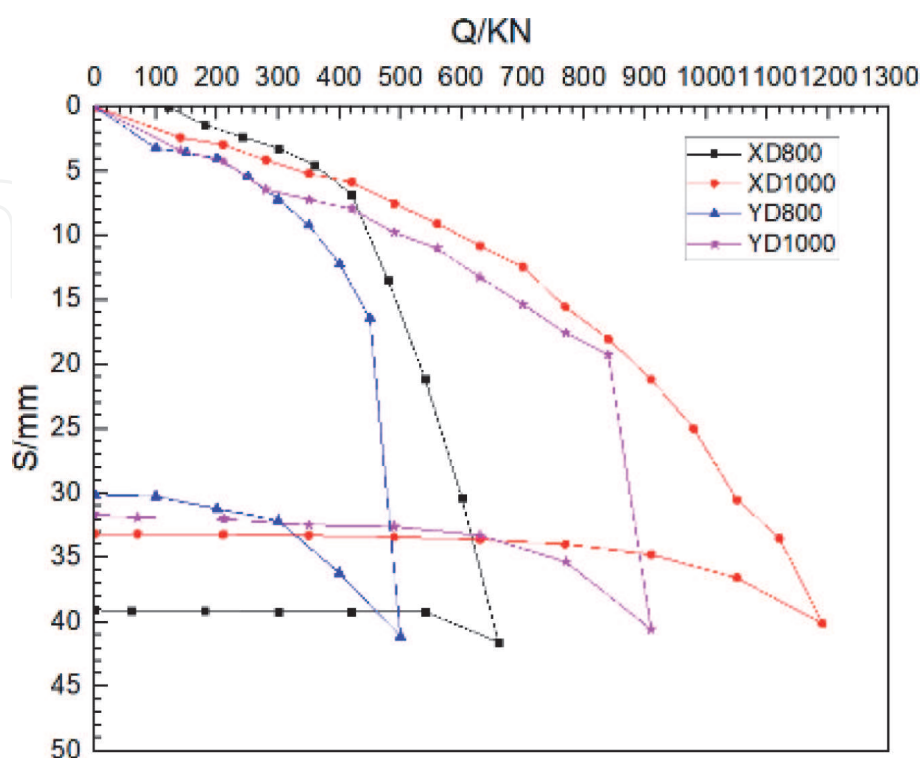
Figure 12.
Q-S curve of the foundation of each pier.

Pier foundation	Q_{cr} (kN)	S_{max} (mm)	Q_u (kN)	S_{qu} (mm)	R_a (kN)	S_{ra} (mm)	Rebound deformation (%)	$\Delta s_e/\Delta s_{e-1}$
YD800	500	41.15	450	16.42	225	4.02	26.8	5.9
XD800	660	41.55	660	41.55	330	3.22	6.0	1.2
YD1000	910	40.56	840	19.25	420	7.95	21.8	12.6
XD1000	1190	40.13	1120	33.50	560	9.09	17.4	2.21

Note: Q_{cr} represents the maximum loading value of pile-soil system failure; S_{max} represents the total settlement at the maximum loading; Q_u represents the ultimate vertical compression bearing capacity of a single pier; S_{qu} means the settlement corresponding to the ultimate bearing capacity; R_a represents the characteristic value of vertical bearing capacity of single pier; S_{ra} represents the settlement corresponding to the characteristic value of bearing capacity; $\Delta s_e/\Delta s_{e-1}$ represents the ratio of the absolute settlement generated by the last loading level to that generated by the upper loading level.

Table 5.
Comparison of foundation analysis data of piers.

for precast pier foundation made of recycled compound concrete, the friction generated between the pier foundation surface and the soil can be ignored. Moreover, the rate of rebound deformation of the precast recycled compound concrete is higher than that of the cast-in-place ordinary concrete pier after unloading. It is mainly due to the precast pier, where the friction between the pier and the soil was insignificant, and consequently, the load transformed to the pier end was relatively larger. Upon the maximum loading, the precast recycled compound concrete pier had larger settlement than the cast-in-situ ordinary concrete pier. As shown in **Table 5**, the $\Delta s_e/\Delta s_{e-1}$ of YD1000 is 12.6, while that of XD1000 is 2.21, indicating that the foundation failure mode of the precast compound concrete pier is different from that of a cast-in-place ordinary concrete pier.

4.2 Load transfer law of pier-soil system

4.2.1 Geological distribution of the test site

The geological distribution of the pier foundation test in the test site is silt in the range of 0.00–0.40 m and sandy soil in the range of 0.40–5.90, respectively.

4.2.2 Load transfer theory of pier-soil system

Based on the load transfer principle of large-diameter single pile without expanding bottom, and relevant literature [34, 35], the load transfer between the pier-soil system includes the following three stages:

1. At the initial stage, the load is mainly undertaken by the friction resistance between pier foundation and soil. The friction resistance of soil at the bottom of the pier does not occur, because of the relative displacement between the bottom of the pier and soil.

2. With the increase of the load, the compression deformation of the whole pier body and the relative displacement between the piers will increase, and thus the friction resistance at the bottom of the pier foundation will gradually increase, and the soil layer at the bottom of the pier will also experience compression settlement with the increase of pier end stress, and the pier end provides part of end resistance.

3. When the load is further increased, the settlement of the pier bottom increases, and correspondingly, the end resistance provided by the pier end increases significantly. On the other hand, with the compression of the soil layer at the pier end, the relative displacement of the piers also increases, and the friction resistance provided by the pier side will further increase.

4.2.3 Analysis of axial force and average friction resistance of pier body

Based on the mechanics of materials that the material satisfies Hooke's law in the elastic deformation range, the relationship between stress and strain could be expressed as Eq. (1).

$$\sigma_c = E_c \times \varepsilon_c \tag{1}$$

where σ_c is the stress of concrete pier foundation, ε_c is the strain of concrete pier foundation, and E_c is the elastic modulus of concrete pier foundation. And the load can be calculated based on the following relationship.

$$N = \sigma_c \times A \tag{2}$$

If the linear expansion coefficient of steel and concrete could be determined by the same deformation together, the cross-section of concrete and steel bar would have the same strain value [36]. In this work, strain gauges placed on the longitudinal bars could serve the internal structure of the pier foundation. Along with the structural reinforcement, six sections are selected on both sides, and six strain gauges are placed on each side (**Figure 6**). By measuring the strain value, the axial force at the section is calculated, and then the distribution of friction resistance at the pier side can be obtained. Under the different levels of load, the axial force distribution diagram of pier body is presented in **Figure 13**.

As shown in **Figure 13**, it can be seen that with the increase of loading load, the axial force of the pier foundation increases. The axial force of the cast-in-place concrete pier foundation decreases with the depth of the pier foundation, indicating that the friction resistance at the pier side plays an important role. When the pier-soil system is damaged, the side resistance of the pier accounts for around 25% of the ultimate compressive bearing capacity. For the precast pier, the lateral resistance is almost zero, which is mainly caused by the gap between the precast pier foundation of compound concrete and the surrounding holes are not easy to be compacted when the undisturbed soil is backfilled.

The friction resistance of the pier body of the cast-in-situ pier foundation is analyzed in the following way: as the height of the test pier foundation is 2.5 m, and the soil layer distributed around the pier foundation has been presented that 0-0.4 m of the pier body is slit, and 0.4–2.5 m of the pier body is medium sand. Under the maximum load, the average friction resistance of the pier body in different soil layers is distributed along the pier body, as shown in **Figure 14**. In addition, with the increase of pier diameter, the greater is the friction resistance of the pier foundation at the same depth, the greater is the vertical compression bearing capacity of the pier foundation.

4.3 Analysis of soil pressure distribution of pier bottom

According to the measurement of the soil pressure distribution of pier bottom foundation, vibrating string earth pressure gauge. During the test, data were read for three to four times with vibrating string sensor readout instrument when each
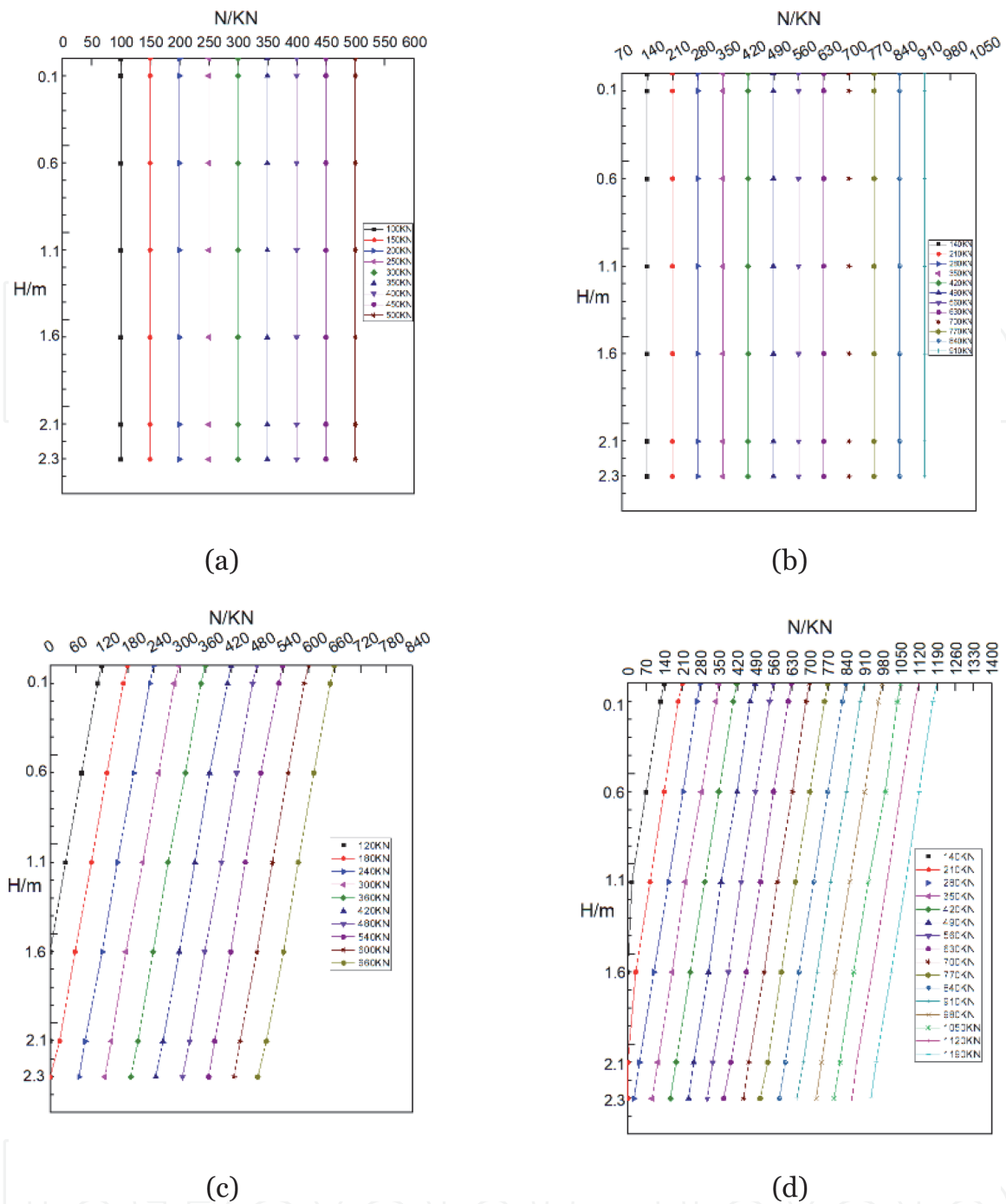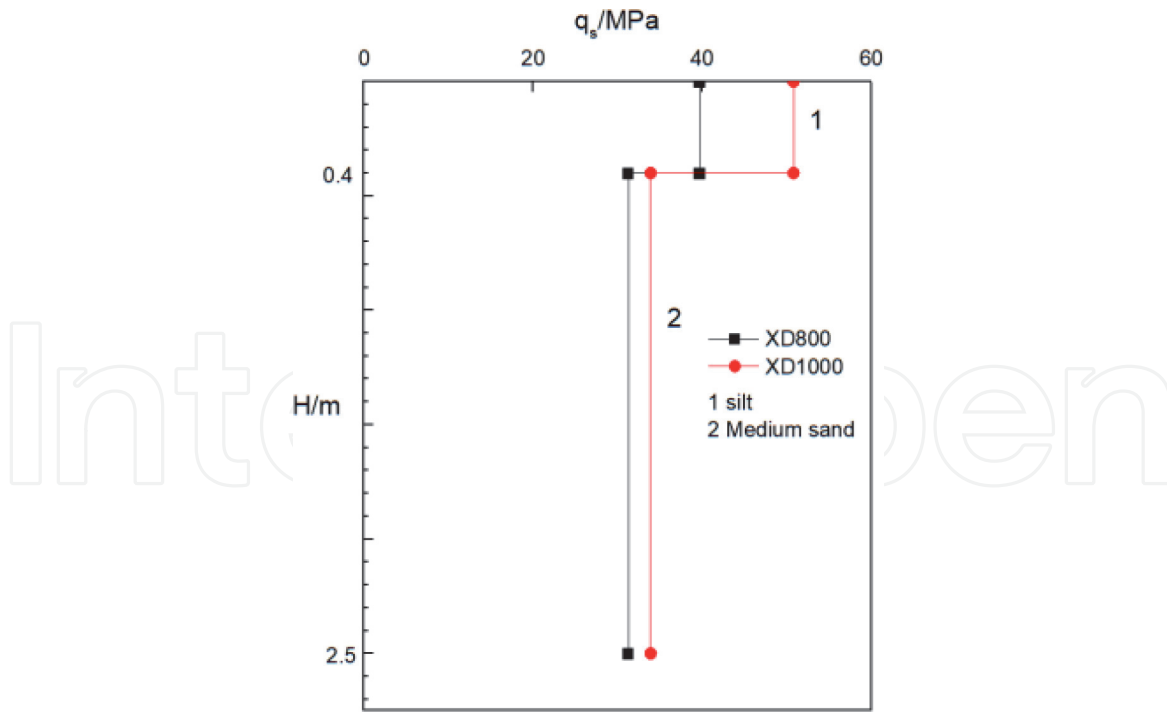
Figure 13.
Axial force distribution of piers. (a) YD800, (b) YD1000, (c) XD800, (d) XD1000.

level of the load was reached, and its average value was taken. The recorded frequency was converted into pressure through Eq. (3):

$$P = K\left(f_i^2 - f_0^2\right) \tag{3}$$

where P is the earth pressure value (MPa), K is the calibration coefficient of the earth pressure gauge (MPa/HZ^2), f_i is the frequency recorded during loading (HZ), and f_0 is the initial frequency (HZ).

Figure 15 presents the measured earth pressure distribution of the foundation at the bottom of the pier. The distribution of soil pressure of precast pier foundation of compound concrete and that of cast-in-place pier foundation of ordinary concrete has the same pattern, that is, the soil pressure of foundation of pier bottom is distributed in a parabolic shape. The main reason is that the bearing layer of the pier

Figure 14.
Average frictional resistance distribution of cast-in-situ concrete piers.

(a)

(b)

(c)

(d)
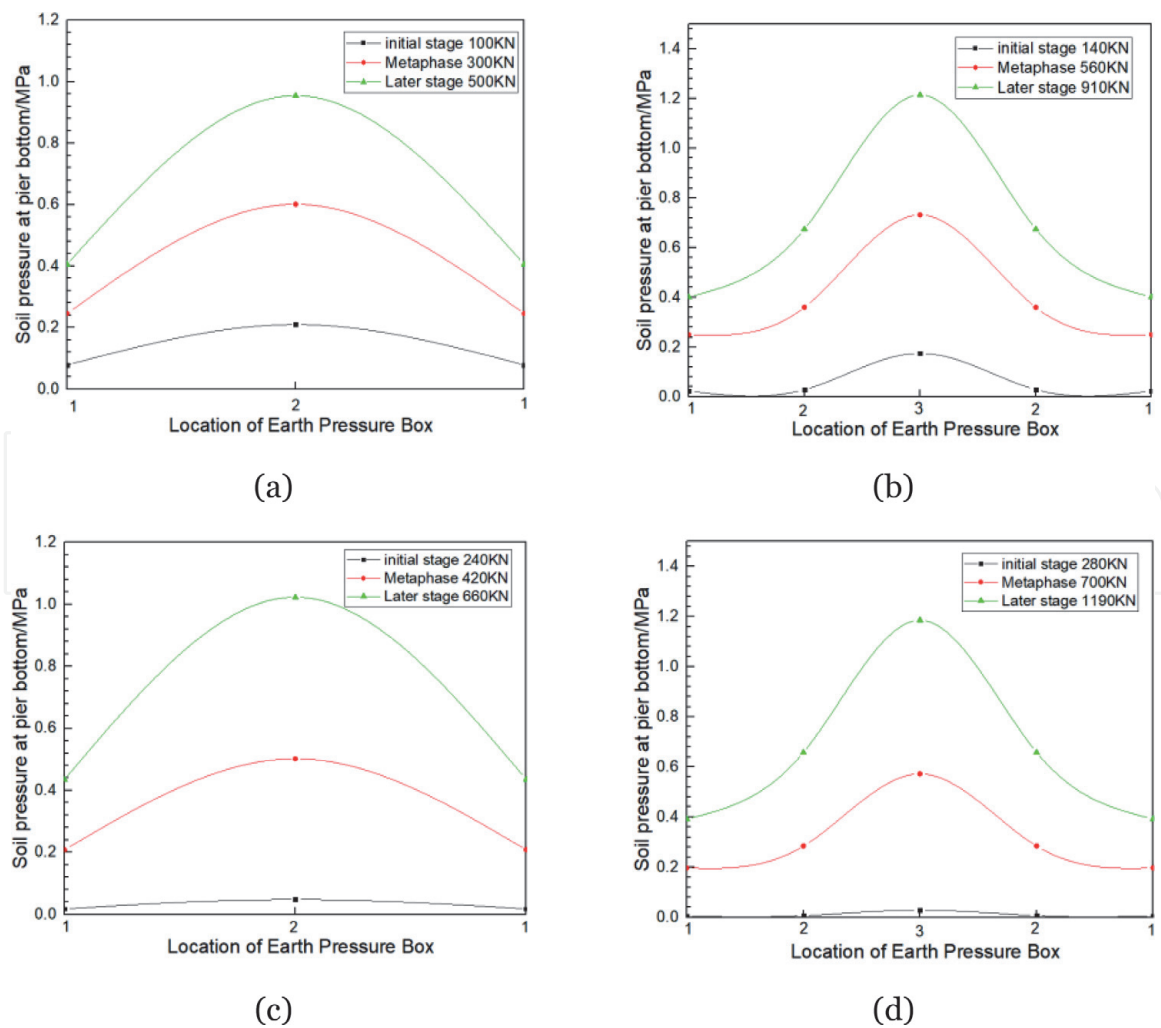
Figure 15.
Distribution of foundation soil pressure at the beginning, middle, and later stage of loading. (a) YD800,
(b) YD1000, (c) XD800, (d) XD1000.

foundation was on the sand soil. In the process of loading, the sand grains at the bottom edge of the pier are easily extruded laterally, and the soil pressure at the edge of the foundation transfers to the middle part, leading to the stress redistribution. As a result, the soil pressure at the edges of the pier bottom was small, while the soil pressure at the middle of the pier bottom was large. At the initial stage of loading, the soil pressure value of the prefabricated pier foundation is much higher than that of the cast-in-place compound concrete pier foundation with the same diameter, which further indicates that the prefabricated pier foundation with recycled compound concrete is almost entirely provided by the resistance at the pier end. Also, with the increase of load, the failure of the bottom edge of the pier was earlier than that of the middle of the pier bottom.

4.4 Failure mode analysis of the pier foundation

The failure modes are presented in **Figure 16**, which the soil of both precast pier foundation and ordinary concrete cast-in-situ pier did not exhibit the bulging damage phenomenon. For precast concrete pier foundation, the settlement increased obviously in the former period, and Q-S curve has obvious turning point (**Figure 12**); therefore, along with the failure mode, the failure belongs to local shear failure damage. For ordinary concrete pier, as the load increases, the soil at the bottom of the pier foundation was compressed. When loaded into the pier-soil system damage, the rate of settlement remained unchanged, and Q-S curve did not show obvious turning point; therefore, along with the failure mode, the failure belongs to piercing-type shear failure forms.

4.5 Research on vertical bearing capacity formula

For the prediction of vertical bearing capacity of pier foundation, according to the analysis of load transfer law of pier-soil system in Section 3.2, it can be seen that the stress form of unexpanded bottom pier foundation tested in this paper is theoretically consistent with that of large-diameter pile foundation. Therefore, the calculation formula of vertical bearing capacity can refer to the code for building pile foundation technology (JGJ 94-2008) [37], specification for design of building

(a) (b)

Figure 16.
Failure modes of concrete piers. (a) Soil around the pier when the precast pier foundation of recycled compound concrete was destroyed, (b) soil around the piers when the foundation of the cast-in-place ordinary concrete was destroyed.

foundation (GB 50007-2011) [38], and literature [29]. In the following section, the feasibility of these calculation formulas is investigated.

4.5.1 Calculation formula of technical code for building pile foundation (JGJ 94-2008)

The formula for calculating the ultimate bearing capacity of a large-diameter single pile can be calculated according to Eq. (4):

$$Q_{uk} = Q_{sk} + Q_{pk} = u \sum \psi_{si} q_{sik} l_i + \psi_p q_{pk} A_p \tag{4}$$

where Q_{sk} stands for total ultimate resistance measured at pile side (kN), Q_{pk} represents the total limit end resistance (kN) of pile side, u is the perimeter (m) of pile body, Ψ_{si} represents the dimensional reduction coefficient of pile lateral resistance (refer to **Table 6**), q_{sik} represents the ultimate lateral resistance (kPa) of the pile side in layer I soil, Ψ_p represents the reduction coefficient of pile tip resistance (refer to **Table 6**), and q_{pk} represents the ultimate end resistance (KPa) with a pile diameter of 800 mm. The reduction coefficients Ψ_{si} and Ψ_p in the formula are calculated according to **Table 6**.

4.5.2 Calculation formula of code for design of building foundation (GB 50007-2011)

The preliminary design of the vertical bearing capacity characteristic value of a single pile is estimated according to Eq. (5):

$$R_a = q_{pa} A_p + u_p \sum q_{sia} l_i \tag{5}$$

where q_{pa} represents the characteristic value of pile tip resistance (kPa), A_p represents the area of pile bottom (m^2), q_{sia} represents the characteristic value of pile lateral resistance (kPa), u_p represents the pile girth (m), and l_i represents the thickness of soil layer i (m).

However, the vertical ultimate bearing capacity of a single pile is divided by safety factor 2, that is, the characteristic value R_a of vertical bearing capacity of a single pile. Therefore, based on this, 2R_a is adopted to calculate the vertical ultimate bearing capacity of a single pile.

4.5.3 Calculation formula in literature

Based on the study in [29], the characteristic value of the vertical bearing capacity of single pier can be calculated by referring to Eq. (6):

$$R_a = \beta f_a A_D \tag{6}$$

where β is the pier foundation correction coefficient, f_a represents the modified characteristic value of foundation bearing capacity of pier base (KPa), and A_D

Soil type	Sand, gravel soil
Ψ_{si}	$(0.8/d)^{1/3}$
Ψ_p	$(0.8/D)^{1/3}$

Note: equal diameter pile d = D.

Table 6.
Dimension reduction factor.

represents the cross-section area of pier, (m2). For the coefficient β, it could be referred to the values in **Table 7**.

The modified characteristic value of foundation bearing capacity of pier base (f_a) in Eq. (6) could be calculated according to Eq. (7):

$$f_a = f_{ak} + \eta_d \cdot \gamma_0 (d - 1.5) \tag{7}$$

where f_{ak} represents the characteristic value of foundation bearing capacity (kPa), η_d refers to the correction coefficient of bearing capacity of foundation considering the buried depth of pier foundation, and γ_0 denotes the depth of the bottom soil of the pier foundation. For groundwater, its effective depth (kN/m^2) d represents the embedded depth of pier foundation (m).

Additionally, the vertical ultimate bearing capacity of a single pile is divided by the safety factor 2, that is, the characteristic value R_a of the vertical ultimate bearing capacity of a single pile. Therefore, $2R_a$ is used to calculate the vertical ultimate bearing capacity of a single pile.

4.5.4 Pier foundation calculation formula selection

Based on Eqs. (4)–(6), **Table 8** shows the comparison of the predicted values and tested results. For the value of Q_{us}/Q_{uj} greater than 1, it indicates that the test value is greater than the calculated value, while for the value of Q_{us}/Q_{uj} less than 1, it indicates that the vertical bearing capacity of pier foundation will be utilized fully

H/D	1.6	1.8	2.0	2.2	2.4	2.6	2.8	3.0
Sandy soil, gravel soil	1.6	1.7	1.8	1.9	2.1	2.3	2.5	2.7

Note: H represents the height of pier foundation, m; D is the diameter of pier foundation, m.

Table 7.
Pier foundation correction coefficient.

Formula	YD800			YD1000			XD800			XD1000		
	Q_{uj}	Q_{us}	Q_{us}/Q_{uj}	Q_{uj}	Q_{us}	Q_{us}/Q_{uj}	Q_{uj}	Q_{us}	Q_{us}/Q_{uj}	Q_{uj}	Q_{us}	Q_{us}/Q_{uj}
JGJ94-2008	400	450	Q1.125	582	840	1.443	661	660	0.998	885	1120	1.265
GB50007-2011	400	450	1.125	628	840	1.337	661	660	0.998	954	1120	1.174
Literature [64]	432	450	1.041	678	840	1.238	645	660	1.023	1013	1120	1.105

Note: Q_{uj} represents the value calculated by the reference formula of vertical ultimate bearing capacity, kN; Q_{us} represents the test value of vertical ultimate bearing capacity under compression, kN.

Table 8.
Comparison of predicted values and test values.

Formula	YD800	YD1000	XD800	XD1000	Average	Mean square error	Coefficient of variation
JGJ94-2008	1.125	1.443	0.998	1.265	1.207	0.191	0.158
GB50007-2011	1.125	1.337	0.998	1.174	1.158	0.140	0.121
Literature [18]	1.041	1.238	1.023	1.105	1.101	0.09	0.09

Table 9.
Statistical characteristics of Q_{us}/Q_{uj} ratio under different calculation formulas.

in the design process. However, it should be noted that the minimum bearing capacity cannot be less than 0.5. Otherwise there will be safety risks and accidents might occur.

The statistical characteristic of the ratio between the test value and the calculated value by different methods are shown in **Table 9**. It can be seen from **Table 9** that the variation coefficient of the formula by Liu [29] is the minimum, indicating that the calculated value of the formula has the minimum fluctuation compared with the experimental value. At the same time, its average value is also the smallest, which is greater than 1, indicating that it is appropriate to calculate the safety reserve.

5. Conclusion

Based on the investigations on the vertical bearing capacity of precast pier foundation filled with demolished concrete lumps, the following conclusions can be drawn:

1. The Q-S curve of prefabricated pier foundation made of recycled compound concrete is of slow deformation when loaded, which is consistent with that of cast-in-place concrete pier foundation. Through Q-S curve, the vertical bearing capacity of prefabricated pier foundation with recycled compound concrete is about 25–30% lower than normal concrete cast-in-situ pier foundation, and in the pier foundation of the same diameter, the rebound deformation of prefabricated pier foundation was higher than that of cast-in-situ pier.

2. With the increase in diameter, the characteristic value of the vertical bearing capacity of the prefabricated foundation made of recycled compound concrete increases. At the same time, when the vertical ultimate bearing capacity of the single pier is reached, the settlement value also increases, which is consistent with the performance law of the cast-in-situ ordinary concrete pier.

3. The load transfer theory of pier-soil system was established, and the accuracy of the theory was verified through experimental analysis. At the same time, the variation rules of axial force, average friction resistance, and the similarities and differences between cast-in-place concrete pier foundation and prefabricated pier foundation made of recycled compound concrete are analyzed by placing strain gauge on longitudinal bars of pier body structure.

4. By placing the earth pressure box at the bottom of the pier, it is analyzed that the prefabricated foundation of DCLs is the same as the cast-in-place foundation of the ordinary concrete. The earth pressure at the bottom of the pier is distributed in a parabola.

5. Based on the comprehensive analysis of the soil pressure distribution and Q-S curve change rule of the foundation at the bottom of the pier, the failure form of the soil mass of the prefabricated pier foundation of recycled compound concrete is local shear failure, while the failure form of the soil mass of the cast-in-situ pier foundation of ordinary concrete is piercing-type shear failure.

6. The method proposed in this study provides a reasonable prediction for the vertical compressive ultimate bearing capacity for both prefabricated pier foundation with recycled compound concrete and cast-in-situ pier foundation of ordinary concrete.

Acknowledgements

Author details

Bin Lei[1,2], Wengui Li[2]*, Zhuo Tang[2] and Fuzhi Yang[2]

1 School of Civil Engineering and Architecture, Nanchang University, Nanchang, Jiangxi, P.R. China

2 Center for Green Technology, School of Civil and Environmental Engineering, University of Technology Sydney, NSW, Australia

*Address all correspondence to: wengui.li@uts.edu.au

IntechOpen

References

[1] Xiao J, Li W, Fan Y, Huang X. An overview of study on recycled aggregate concrete in China (1996-2011). Construction and Building Materials. 2012;**31**:364-383. DOI: 10.1016/j. conbuildmat.2011.12.074

[2] Li W, Sun Z, Luo Z, Shah S. Influence of relative mechanical strengths between new and old cement mortars on the crack propagation of recycled aggregate concrete. Journal of Advanced Concrete Technology. 2017;**15**(3): 110-125. DOI: 10.3151/jact.15.110

[3] Lei B, Li W, Tam V, Sun Z. Investigation on properties of RAC under coupling loading and freeze-thaw cycles in salt-solution. Construction and Building Materials. 2018;**163**: 840-849. DOI: 10.1016/j. conbuildmat.2017.12.194

[4] Li W, Luo Z, Long C, Wu C, Duan W, Shah S. Effects of nanoparticle on the dynamic behaviors of RAC under impact loading. Materials and Design. 2016;**112**:58-66. DOI: 10.1016/j. matdes.2016.09.045

[5] Lei B, Li W, Li Z, Wang G, Sun Z. Effect of cyclic loading deterioration on concrete durability: Freeze-thaw and carbonation. Journal of Materials in Civil Engineering. 2018;**30**(9): 04018220. Available from: http://hdl.ha ndle.net/10453/131532

[6] Li W, Xiao J, Sun Z, Kawashima S, Shah S. Interfacial transition zones in recycled aggregate concrete with different mixing approaches. Cement and Building Materials. 2012;**35**: 1045-1055. DOI: 10.1016/j.conbuildmat. 2012.06.022

[7] Li W, Chu L, Tam W, Poon C, Duan W. Effects of nano-particles on failure process and microstructural properties of recycled aggregate concrete. Construction and Building Materials. 2017;**142**:42-50. DOI: 10.1016/j.conbuildmat.2017.03.051

[8] Wu B, Jian S, Zhao X. Structural behavior of steel-concrete partially encased composite columns containing demolished concrete lumps under axial compression. Engineering Structures. 2019;**197**(15):1-18. DOI: 10.1016/j. engstruct.2019.109383

[9] Wu B, Yu Y, Zhao X. Residual mechanical properties of compound concrete containing demolished concrete lumps after exposure to high temperatures. Fire Safety Journal. 2019; **105**:62-78. DOI: 10.1016/j. firesaf.2019.02.008

[10] Wu B, Yu Y, Chen Z, Zhao X. Shape effect on compressive mechanical properties of compound concrete containing demolished concrete lumps. Construction and Building Materials. 2018;**187**:50-64. DOI: 10.1016/j. conbuildmat.2018.07.086

[11] Wu B, Li Z. Mechanical properties of compound concrete containing demolished concrete lumps after freeze-thaw cycles. Construction and Building Materials. 2017;**155**:187-199. DOI: 10.1016/j.conbuildmat.2017.07.150

[12] Zhou L. The study about of belled pier found on deformation modulus of bearing stratum [thesis]. Xi'an University of Architecture and Technology; 2013 (in Chinese)

[13] Zhao Z, Fu Z. Discussion of working mechanism on pier foundation. Soils and Foundations. 2004;**2**:49-50 (in Chinese)

[14] Zhang J, Wang J. Analysis is and design of belled pier foundation. Chinese Journal of Geotechnical Engineering. 1996;**3**:67-73 (in Chinese)

[15] Wang F, Wang M. Working mechanism and bearing capacity design

of the pedestal pier with large diameter. Chinese Journal of Geotechnical Engineering. 2002;**2**:251-253 (in Chinese)

[16] Hoang N, Liao K, Tran X. Estimation of scour depth at bridges with complex pier foundations using support vector regression integrated with feature selection. Journal of Civil Structural Health Monitoring. 2018;**8**(3):431-442. DOI: 10.1007/s13349-018-0287-2

[17] Liu Y, Guo L, Zhang Q, et al. Study on the calculation method of vertical bearing capacity of pier foundation. Sichuan Building Materials. 2010;**36**(4):50-52 (in Chinese)

[18] Ha J, Ko K, Jo S, Park H, Kim D. Investigation of seismic performances of unconnected pile foundations using dynamic centrifuge tests. Bulletin of Earthquake Engineering. 2019;**17**(5):2433-2458. DOI: 10.1007/s10518-018-00530-y

[19] Sego D, Biggar K, Wong G. Enlarged base (belled) piles for use in ice or ice-rich permafrost. Journal of Cold Regions Engineering. 2003;**17**(2):68-88. DOI: 10.1061/(ASCE)0887-381X(2003)17:2(68)

[20] Jiang J, Gao G. Study on modifying coefficient of end-bearing resistance of large diameter belled piles. Rock and Soil Mechanics. 2006;**12**:2282-2288 (in Chinese)

[21] Liu Z, Jiang Y, Gong W. Discussion of the design method of large diameter belled pile's bearing capacity according to settlement. Journal of Southeast University (Natural Science Edition). 2001;**4**:49-53 (in Chinese)

[22] Lee C. Settlement and load distribution analysis of underreamed piles. ARPN Journal of Engineering and Applied Sciences. 2007;**2**(4):35-40

[23] Liu Z, Zhu F, Lu T, et al. Bearing capacity test of pier foundation in cohesive soil. Journal of Shenyang Jianzhu University Natural Science. 2008;**5**:783-787 (in Chinese)

[24] Liu Z, Shan M, Wang S, et al. Research of pier foundation on cohesive soil. Concrete. 2009;**2**:42-44 (in Chinese)

[25] Morici M, Minnucci L, Carbonari S, Dezi F, Leoni G. Simple formulas for estimating a lumped parameter model to reproduce impedances of end-bearing pile foundations. Soil Dynamics and Earthquake Engineering. 2019;**121**:341-355. DOI: 10.1016/j.soildyn.2019.02.021

[26] Peter J, Lakshmanan N, Devadas MP. Investigations on the static behavior of self-compacting concrete under-reamed piles. Journal of Materials in Civil Engineering. 2006;**18**(3):408-414. Available from: https://ascelibrary.org/doi/10.1061/(ASCE)0899-1561(2006)18:3(408)

[27] Liu Z, Zhu F, Shu Z, et al. Research on horizontal bearing capacity of widen-bottom non-reinforced concrete pier foundation on cohesive soil. Journal of Liaoning Technical University(Natural Science Edition). 2008;**6**:850-852 (in Chinese)

[28] Liu Z. Experimental study on bearing capacity of pier-type foundation with sand soil and gravel. Geotechnical Investigation & Surveying. 1996;**3**:9-12 (in Chinese)

[29] Liu Z. Experimental investigation of non-reinforced concrete pier foundation [thesis]. Nanjing: Northeastern University; 2009 (in Chinese)

[30] JGJ225T-2010. Technical specification for large diameter bored pile. Beijing: China Building Industry Press; 2010 (in Chinese)

[31] Zhang J, Wu Y, Xu Y, et al. Basic engineering testing technology and case analysis. Beijing: Science Press; 2012 (in Chinese)

[32] JGJ106–2014. Technical specification for foundation pile inspection[S]. Beijing: China Building Industry Press; 2014 (in Chinese)

[33] Wang Z. Comparison of design between manual bored pile and pier foundation. Sichuan Architecture. 2010; **30**(06):94-95 (in Chinese)

[34] Zhou H, Chen Z. Analysis of effect of different construction methods of piles on the end effect on skin friction of piles. Frontiers of Architecture and Civil Engineering in China. 2007;**1**(4): 458-463

[35] Huo Z. Calculation of vertical bearing capacity of pile with manual hole digging and bottom expanding [thesis]. Xi an: Chang 'an university; 2002 (in Chinese)

[36] Tong J, Lin S, Dai Y. Load transfer behavior of large bore bored piles. Chinese Journal of Geotechnical Engineering. 1994;**06**:123-131 (in Chinese)

[37] JGJ 94–2008. Technical specification for building pile foundation. Beijing: China Building Industry Press; 2008 (in Chinese)

[38] GB 50007–2011. Code for design of building foundations. Beijing: China Building Industry Press; 2011 (in Chinese)